Ion-irradiation-induced selective bond rearrangements in amorphous GeTe thin films

R. De Bastiani,[1,*] E. Carria,[1] S. Gibilisco,[1] M. G. Grimaldi,[1] A. R. Pennisi,[1] A. Gotti,[2] A. Pirovano,[2] R. Bez,[2] and E. Rimini[3]

[1]*Dipartimento di Fisica ed Astronomia, Università di Catania and MATIS CNR-INFM, 64 via S. Sofia, I-95123 Catania, Italy*

[2]*Numonyx, R&D Technology Development, Via Olivetti 2, Agrate Brianza, 20041 Milan, Italy*

[3]*Dipartimento di Fisica ed Astronomia, Università di Catania and CNR-IMM, 64 via S. Sofia, I-95123 Catania, Italy*

(Received 24 July 2009; revised manuscript received 11 November 2009; published 9 December 2009)

The change in the local order of amorphous sputter deposited GeTe thin films irradiated with Ge^+ ion and its influence on the subsequent thermal induced crystallization has been investigated by means of micro-Raman spectroscopy and *in situ* time-resolved reflectivity. A reduction in the Ge-rich tetrahedral species and an enhancement of the crystallization kinetics occurred in the irradiated amorphous samples. The rearrangement of the amorphous network is suggested to be related to thermal spikes effects rather than to the defects produced by the ions in the collision cascade.

DOI: 10.1103/PhysRevB.80.245205 PACS number(s): 61.43.Dq, 78.30.−j, 61.80.Jh, 64.70.−p

I. INTRODUCTION

The GeTe system belongs to IV-VI compound semiconductor and it is characterized by fast crystallization[1] and high stability of the amorphous phase.[2] GeTe is the basic ingredient of a class of materials, GeTe-Sb_2Te_3 ternary alloys,[3] employed as the active medium in optical and electrical data storage devices.[4] In these materials, the phase change data storage concept is based on the huge change in the optical and electrical properties associated to the reversible amorphous to crystal transition induced by laser or electrical current pulse. In both cases, the energy pulse locally melts the processed material to write an amorphized region by fast quench or heats it above its crystallization temperature but below the melting temperature to crystallize the material (erase). The crystallization time of the phase change material is the data-rate limiting factor. One of the main issue that has to be stated for the development of data storage devices is the link between the local order in the amorphous phase and its stability. In fact, it is known that, for a given alloy composition, several amorphous states exist, and each one is characterized by a different crystallization velocity. For example, crystallization of a melt-quenched $Ge_2Sb_2Te_5$ (GST) amorphous is an order of magnitude faster than that of the sputter deposited amorphous.[5] Differences in the crystallization velocity have been observed in amorphous relaxed by low-temperature annealing.[6] It is known that ion implantation is a tool to modify in a controlled way the amorphous state,[7] and it has been recently reported a faster crystallization in ion-irradiated amorphous GST films with respect to the unirradiated samples.[8,9] Moreover, it has been shown that ion implantation in GST layers causes a densification of the structure.[9]

The different, if any, local order of the amorphous structures, which may be responsible for the different crystallization speed is quite difficult to identify and quantify experimentally in ternary alloys because of the variety of parameters that can play a role in the analysis and in the comparison with simulation. For this reason, the binary GeTe system is of interest since it could be taken as a model for the more complex ternary and higher-order alloy compositions. In this work, we examine the effect of ion irradiation and thermal annealing on the local order of amorphous GeTe thin films, mainly by means of micro-Raman spectroscopy.

II. EXPERIMENTAL PROCEDURE

GeTe amorphous films, 40 nm thick, were prepared by rf sputter deposition at room temperature (RT), from a stoichiometric target, over oxidized Si wafers. Samples were irradiated at RT with 130 keV Ge^+ ions at several fluences in the range between 1×10^{13}–1×10^{15} ions/cm^2. The beam current was kept constant to 100 nA to avoid heating of the sample. The ions projected range, by SRIM (Ref. 10) calculations, is ~54 nm ($\Delta R_P\sim24$ nm). The dose and the beam energy were chosen in such a way to avoid any appreciable change in the stoichiometry of the sample and to provide a nearly uniform energy loss (~1.35 keV ion^{-1} nm^{-1}) in nuclear encounters, across the sample. Some samples were implanted at the liquid-nitrogen temperature (LN_2) to ascertain the influence of irradiation-induced defects recombination. Moreover, some implants were performed through a mask to make more reliable the comparison between irradiated and unirradiated zones. Room-temperature unpolarized micro-Raman spectra were recorded in a backscattering geometry using a single spectrometer. The GeTe samples were excited with a He-Ne laser ($\lambda=633$ nm), focused to ~2 μm using a microscope objective lens. The incident laser power was adjusted to 2 mW in order to minimize heating effects in the illuminated sample region. In particular, according to our experimental setup we estimate for a-GeTe a temperature increase $\Delta T\approx40$ °C for 300 s acquisition time. The crystallization of unirradiated and irradiated amorphous films was followed by *in situ* time-resolved reflectivity (TRR) using a low power He-Ne laser probe during annealing at 163 °C at a pressure of about 10^{-3} Torr. The heating rate was 10 °C/min and the settled temperature was constant within ±0.1 °C. The chemical composition of the amorphous and annealed GeTe films has been evaluated by 2.0 MeV He^+ Rutherford backscattering spectrometry. The stoichiometry resulted $Ge_{0.54}Te_{0.45}$ (~1% of Ar contamination) and re-

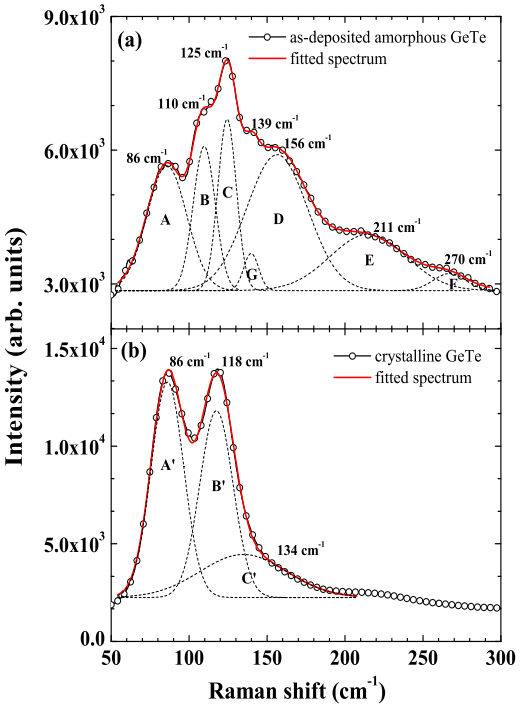

FIG. 1. (Color online) (a) Raman spectrum of amorphous GeTe thin films (open circles) and representative fitting (red curve) with seven Gaussian distributions (dashed lines). The G band, centered at 139 cm^{-1}, was employed in the fitting procedure to increase the quality. (b) Spectral deconvolution (red curve) of the crystalline GeTe Raman spectrum (open circles).

mained practically unchanged after implantation and/or annealing.

In order to obtain complementary information related to the crystallization process, transmission electron microscopy (TEM) analyses in plan-view configuration, were performed on partially crystallized preirradiated amorphous GeTe films, using a JEOL JEM 2010F TEM/STEM equipped with a 200 kV Schottky field emission electron gun and an ultrahigh-resolution objective lens pole piece. The morphology of implanted GeTe samples was investigated by atomic force microscopy (AFM) analyses using a Digital Instruments Microscope Dimension 3100 in high amplitude mode with ultrasharpened Si tips.

III. RESULTS AND DISCUSSION

The Raman spectrum of the as-deposited amorphous GeTe is reported in Fig. 1(a) (open circles). The fit of the spectrum (continuous line) required six main Gaussian contributions, denoted A, B, C, D, E, and F, visible in the same figure (dashed lines). The fitting parameters (peak position, width, and normalized area) of the raw Raman data are summarized in Table I. The positions of the Gaussian curves are in a good agreement with the Raman bands previously observed for GeTe compounds.[11,12] The presence in the spectrum of an additional band at ~139 cm^{-1} (G peak) has been attributed to the aging of the sample. In fact, our samples suffered considerable oxidation, during intermediate periods of exposure to air and the G band becomes more intense in dated samples. All the measurements reported in this work have been performed within one month from the film deposition.

It has been reported that the tetrahedral species of the type $GeTe_{4-n}Ge_n$ ($n=0,1,2,3,4$) are the main building blocks of the GeTe glass structure.[11] Assuming that the concentration of the tetrahedral species follows a purely statistical rule as described by the random bonding model,[13] the distributions of these types of tetrahedral, for the measured sample stoichiometry, consist of 4.1% $GeTe_4$, 20% $GeTe_3Ge$, 36.75% $GeTe_2Ge_2$, 30% $GeTeGe_3$, and 9.15% $GeGe_4$. On the basis of previous investigation,[11,12] focused on the analysis of the temperature-reduced Raman spectra, the Raman bands of the amorphous GeTe phase have been assigned. The broad A band can be attributed to the overlap between the bending modes of the tetrahedra[11] and the disordered Te chains.[14] The B band and the C band correspond to vibrational bands of corner-sharing tetrahedral units $GeTe_{4-n}Ge_n$ with $n=0,1$ (Te-rich) and $n=2,3$ (Ge-rich) tetrahedral species, respectively.[12] The higher intensity of the C band compared to the B band is probably due to the distributions of these types of tetrahedra with proportions ~66.75% and 24.1%, respectively. The strong intensity and amplitude of the D band might result from several contributions. One of them[12] could be the edge sharing of the $GeTe_4$ unit. However, the low abundance (~4.1%) of the $GeTe_4$ unit cannot account for the high intensity of the D band and a contribution from a further mode must be considered. The D band is very close to those observed in amorphous GeTe by coherent phonon

TABLE I. Peak parameters (peak position, width, and normalized area), as determined through fits of the experimental data of as deposited, irradiated, and (unirradiated) partially crystallized amorphous GeTe.

Sample	As deposited		Irradiated		Partially crystallized	
Peak identity	Peak position (cm^{-1})	FWHM (cm^{-1})	Norm. peak area	FWHM (cm^{-1})	Norm. peak area	FWHM (cm^{-1})	Norm. peak area
A	86	25.5	20	25	17.5	25	18
B	110	14	13	15.5	12.5	15.5	12.5
C	125	12	13.5	14.5	10.5	14	10.5
D	156	36	34	40	35	40	34.5
E	211	49	17.5	53	22	53	22
F	270	22	2	25	2.5	25	2.5

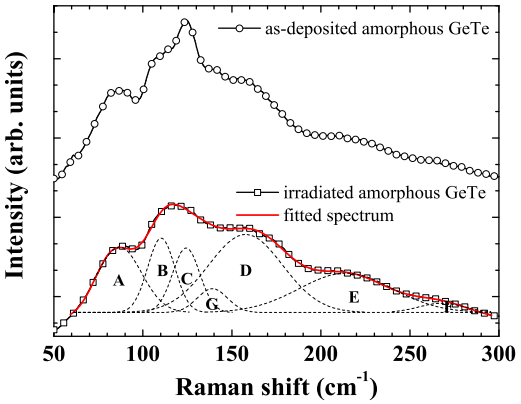

FIG. 2. (Color online) Comparison between the Raman spectra of the unirradiated (open circles) and irradiated amorphous (open squares) GeTe. The latter was fitted (red curve) assuming seven Gaussian distributions (dashed lines).

spectroscopy[15] and it was interpreted as a mode due to small percentage of disordered Te chains. Moreover, partial radial distribution functions of amorphous GeTe films revealed that GeTe samples have striking long-range correlations of Te atoms[16] up to 10 Å. We propose that the D band includes the vibrational density of states of a disordered arrangement of long Te chains since the proper characteristic energy for vibrations of the Te chains in amorphous tellurium[14] is $\sim 157\ \mathrm{cm}^{-1}$. The large E band may be assigned to antisymmetric stretching modes of the tetrahedra.[11] Finally, the F band is consistent with the signal from Ge-Ge bonds in amorphous Ge.[11]

The spectrum of the crystalline GeTe, reported in Fig. 1(b), shows two main contributions of similar intensities at $86\ \mathrm{cm}^{-1}$ (A′) and $118\ \mathrm{cm}^{-1}$ (B′), respectively. The crystalline GeTe was obtained by annealing at 163 °C for 2 h. The fit of the spectrum, in the 50–200 cm^{-1} range (red curve), required an additional Gaussian (C′) centered at $134\ \mathrm{cm}^{-1}$. This band is likely due to the Te chain vibration whose energy shifts from $155\ \mathrm{cm}^{-1}$ in amorphous GeTe to lower frequencies in the crystalline phase because of the long-range interactions between ordered chains.[14]

The Raman spectrum of amorphous GeTe irradiated with Ge ions at fluence $1\times10^{14}\ \mathrm{cm}^{-2}$ is reported in Fig. 2 (open squares). The spectrum of the unirradiated amorphous is shown for comparison (open circles). The experimental data of the irradiated sample was fitted (red line) with the six bands indicated in Table I. The fit was obtained assuming an increase in the full width at half maximum of about 10% for each Gaussian contribution. The spectrum of the irradiated amorphous GeTe shows remarkable changes in the relative intensity of the strongest Raman bands ascribed to the $GeTe_{4-n}Ge_n$ tetrahedral units. In particular a decrease in the lighter Ge-rich ($n=2,3$) tetrahedral species could be the cause of the reduction in the C band. These modifications are associated to a reduction in the amorphous stability as detected by *in situ* TRR measurements during annealing at 163 °C.

Figure 3(a) shows the reflectivity signal during the annealing, for as-deposited unirradiated (open circles) and irradiated amorphous GeTe films at fluence of $1\times10^{14}\ \mathrm{cm}^{-2}$ at

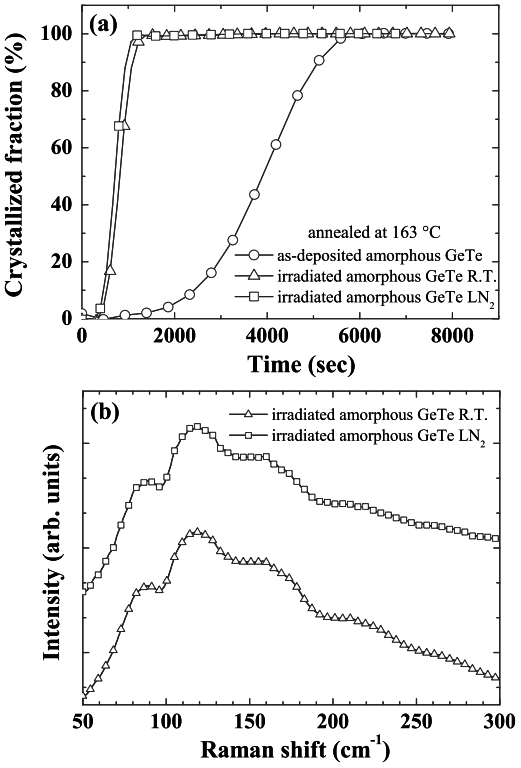

FIG. 3. (a) Reflectivity vs annealing time at 163 °C for as-deposited amorphous (open circles) and Ge^+ irradiated amorphous films at a fluence of $1\times10^{14}\ \mathrm{at./cm}^2$ performed at room (open triangles) or liquid-nitrogen temperature (open squares). (b) Raman spectra of Ge^+ irradiated amorphous GeTe films, at a fluence of $1\times10^{14}\ \mathrm{at./cm}^2$, performed at room (open triangles) and liquid-nitrogen temperature (open squares).

room (open triangles) or liquid-nitrogen temperature (open squares). The zero of the time scale is the time at which the settled temperature is reached. In the unirradiated GeTe the reflectivity remains initially constant up to about 15 min. After this transient it increases abruptly and saturates at the crystalline value when the crystallization is complete and the polycrystalline phase is formed. A similar trend occurs in the irradiated samples although the overall transformation time is considerably reduced. Therefore, TRR measurements indicate that the crystallization process is faster in the implanted amorphous layer with respect to the unirradiated film. The temperature during irradiation does not affect the crystallization kinetics as can be inferred from the TRR curves shown in Fig. 3(a) relatives to samples implanted under the same conditions at different temperatures (77 and 300 K). Moreover, amorphous layers implanted at liquid-nitrogen temperature show the same local order as observed after irradiation at room temperature [Fig. 3(b)]. This unambiguously demonstrates that any dynamic annealing process occurring during the implantation does not change the density of the defects responsible for the crystallization enhancement and that the main effect of irradiation is associated to the prompt regime of the collision cascade and not to the delayed effect, influenced by the movement of the displaced atoms.

Figure 4 reports the incubation time τ as a function of the irradiation fluence in preirradiated amorphous GeTe films (in

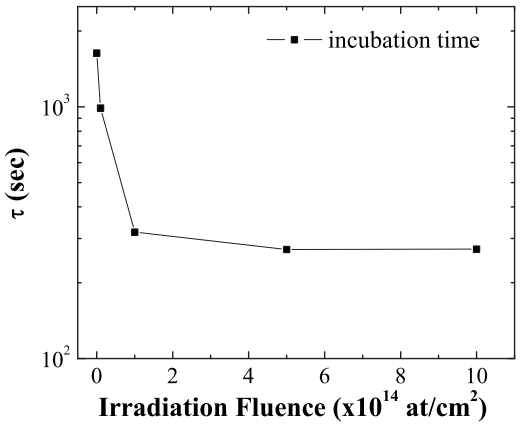

FIG. 4. Incubation time τ versus implantation fluence in preirradiated amorphous GeTe films. The samples were annealed, after a constant heating rate, at 163 °C. The incubation time was experimentally measured as the elapsed time until the reflectivity signal increases by 10% of its initial value during the thermal treatment.

the range between $1\times10^{13}-1\times10^{15}$ ions/cm^2), measured during annealing at 163 °C by means of TRR analysis. The incubation time, necessary to establish a steady-state nucleation, is here assumed to be the elapsed time until the reflectivity signal increases by 10% of its initial value. The incubation time of preirradiated amorphous films is dramatically enhanced compared to the unirradiated GeTe sample. In particular, by increasing the irradiation fluence τ exhibits an abrupt decreases until a saturation value for an implantation fluence of 1×10^{14} ions/cm^2. To directly compare unirradiated and irradiated amorphous, some samples were prepared implanting 130 keV Ge^+ ions at the saturation fluence of 10^{14} ions/cm^2 through a mask consisting of a copper grid, with holes and bar width of 36 and 25 μm, respectively, placed at the sample surface. In this way selectively implanted regions next to unimplanted areas were formed. Figure 5 shows a sequence of bright-field TEM image of the film surface after anneal at 163 °C for several times. At this temperature, crystallization occurs mainly inside the ion-irradiated area and only at later time grains nucleate in the unirradiated region. Even the growth velocity is enhanced in the irradiated regions, the growth stops at the boundary with the unirradited area [see Fig. 5(c)]. The effect of the irradiation on the film density has been evaluated by measuring the

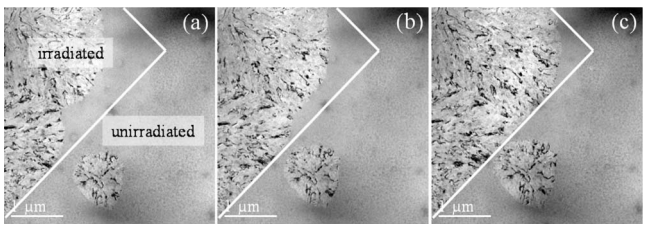

FIG. 5. TEM plan-view micrographs of as-deposited amorphous GeTe films, implanted with 130 keV Ge^+ ions at 1×10^{14} at./cm^2, after (a) 15 min, (b) 16 min, and (c) 17 min anneal performed at 163 °C. The presence, during implantation, of a copper mask placed on the sample surface has produced selectively implanted areas next to not-implanted areas.

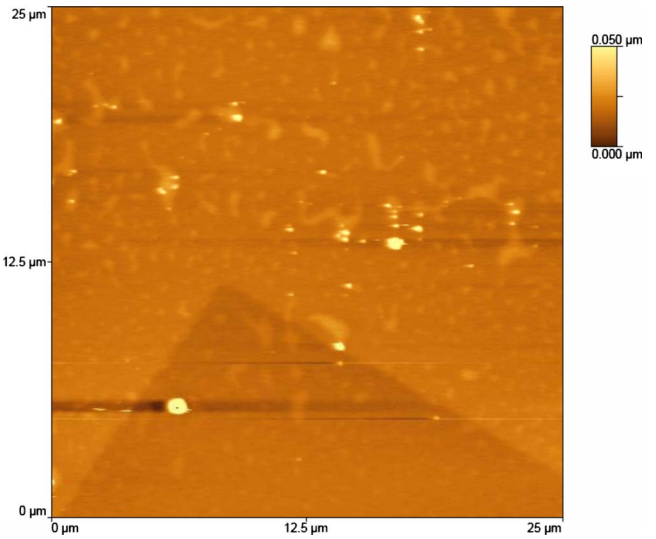

FIG. 6. (Color online) Representative AFM images for as-deposited amorphous GeTe films implanted, through a mask grid, with 130 keV Ge^+ ions at 1×10^{14} Ge/cm^2. Irradiated regions are depressed of 3 nm compared to those not exposed to the ion beam.

step height (by atomic force microscopy) in a sample implanted through the mask grid. The AFM image of the irradiated region, shown in Fig. 6, indicates that the ion beam induces a reduction in the film thickness observed as a depression, of about 3 nm (i.e., 7%), with respect the surface of the unirradiated regions. This vertical shrinkage is comparable to that occurring during the crystallization of GeTe due to the different density of the deposited amorphous and crystalline phases (not shown). In the crystalline phase Ge atoms are reported to switch from tetrahedrally coordinated to octahedrally coordinated sites.[17] In fact, an octahedral coordination requires a lower volume than a fourfold tetrahedral coordination. The densification of the amorphous generated by the ion irradiation reduces considerably the mechanical stress during the phase change in line with the enhancement of the crystallization measured in the implanted samples. No densification effect was observed in implanted amorphous Ge samples for an irradiation fluence of 1×10^{14} Ge/cm^2.

To get more insights in the role played by the $GeTe_{4-n}Ge_n$ tetrahedral species on the mechanism of the amorphous to crystal GeTe phase transition, we measured the Raman spectrum of amorphous regions in a partially transformed sample in which the crystalline fraction (detected by TRR) amounts to 20%. The optical micrograph reported in the inset of Fig. 7, shows that the annealed sample consists of crystalline islands (white regions) embedded in an amorphous matrix (gray area). Crystalline and amorphous areas are clearly visible due to the large optical contrast between the two phases. Micro-Raman measurements were performed on both crystalline and amorphous regions, of the partially crystallized layer. The resulting spectra are reported in Fig. 7. The spectra of the white regions (open circles) is typical of the crystalline GeTe film reported in Fig. 1(b). Vice versa, the spectra collected in gray regions (open squares) differ from that of the as deposited and are similar (Table I) to the Raman spectrum of the irradiated amorphous films shown in Fig. 2, indicating

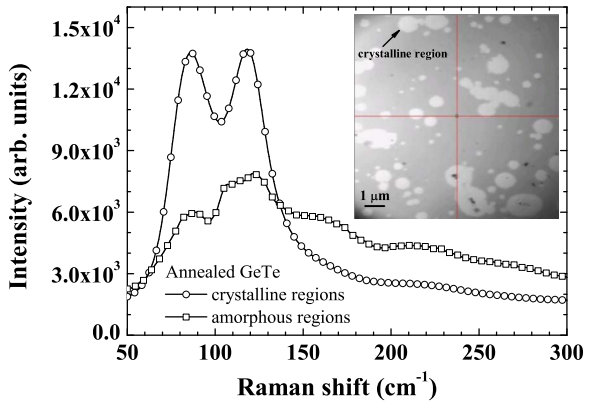

FIG. 7. (Color online) Micro-Raman spectra of (unirradiated) partially crystallized GeTe sample collected in the amorphous (open squares) and crystalline (open circles) regions. The inset reports an optical micrographs of the annealed amorphous GeTe film with a surface crystalline fraction of ~20%.

that appreciable structural rearrangements took place in the amorphous network at the early stage of the phase transition. In order to exclude the presence of submicrometric crystalline grains in the amorphous regions, the same partially transformed sample was analyzed by transmission electron microscopy (not shown). No crystalline regions could be detected in the 200 μm^2 sampled amorphous area, being 30 nm the minimum detectable crystalline size.

IV. PHENOMENOLOGICAL MODELING

It is known that the fraction of the tetrahedral species that constitute the glass structure of GeTe film progressively changes, during the heating, in such a way to form Te-rich tetrahedra at the expense of Ge-rich tetrahedra.[11,17] The increased number of Te atoms in the first coordination cell of Ge facilitate the formation of $GeTe_6$ octahedra that are the basic units of the crystalline GeTe. Similarly, in the irradiated amorphous samples, the reduction in Ge-rich tetrahedra with respect to the Te-rich tetrahedral, promotes the system to a state closer to the crystalline structure. This intermediate state, prior to the crystallization process, is probably achieved by ion-induced thermal spike effects. In dense collision cascade at the end of the displacements spike, the energy is dissipated as lattice vibration or heat. The duration of the thermal spike can be estimated as $t \sim r^2/4D_T$, where r is the dimension of the collision cascade and D_T the thermal diffusivity of the target ($\sim 3.2 \times 10^{-2}$ cm^2/s) (Ref. 18). Assuming as an order of magnitude a radius r of about 10 nm, characteristic of the collision cascade lateral extension at the adopted projectile mass and energy and target composition, the quenching time or duration of the thermal spike amounts to $\sim 10^{-11}$ s. The typical crystallization times in several chalcogenides (GST, GeTe) run from hours at low temperatures (~150 °C) to few hundredth nanoseconds at temperatures below the melting point. The process is thermally activated with an energy of about 2 eV. These values imply a huge pre-exponential factor[19] in all the rate (nucleation rate, crystal growth), orders of magnitude higher than that observed in semiconductors. The same factor might be invoked to justify the ion-induced effect here reported. For diffusion limited crystallization, the grain growth velocity u is related to the atomic diffusivity D in the amorphous by $u = f_S 6D/\lambda$, where λ is the average interatomic distance and $f_s < 1$ is the fraction of sites where a new atom can be incorporated. The measured grain growth velocity of the GeTe, by Lu and Libera (Ref. 20) gives $u = 5.9(\pm 0.5) \times 10^{23}$ (nm/s)exp(-1.77 eV/k_BT). Assuming that a local bond rearrangement from the Ge-rich tetrahedra to the Te-rich tetrahedra, requires a diffusivity of 0.5 nm during the lifetime of the thermal spike, a temperature of ~870 K is needed. The melting point of GeTe (Ref. 21) is 1003 K, well above the previous estimate. A general feature of the crystallization process of amorphous (deposited or Ge implanted) chalcogenides is that the extremely high growth velocity implies an atomic-diffusion coefficient on the order of 10^{-4} cm^2/s. A value typical of diffusivity in the liquid is unlikely for a solid material and this could be an indication that collective atomic rearrangement plays a key role in the crystallization of these materials.

V. CONCLUSIONS

In conclusion, we have analyzed by micro-Raman spectroscopy and TRR measurements the effect of ion irradiation and thermal annealing on the local order of amorphous GeTe thin films. A correlation between the amorphous GeTe phase stability and the percentage of Ge-Te bonds has been presented. The structure of GeTe, as determined by Raman spectroscopy, shows interesting alterations after irradiation, similarly to that observed in partially crystallized GeTe samples, with a strong decrease in the contribution of Ge-rich tetrahedra and the formation of an intermediate structural order between the amorphous and the crystalline phases.

ACKNOWLEDGMENTS

The authors thank F. Ruffino and F. Giannazzo for AFM analysis, C. Bongiorno for TEM analysis. Work supported by FIRB Project-BIP06Y5JJ.

*riccardo.debastiani@ct.infn.it

[1] M. Chen, K. A. Rubin, and R. W. Barton, Appl. Phys. Lett. **49**, 502 (1986).

[2] M. Okuda, H. Naito, and T. Matsushita, Jpn. J. Appl. Phys., Part 1 **31**, 466 (1992).

[3] N. Yamada, Proc. SPIE **3109**, 28 (1997).

[4] A. Pirovano, A. L. Lacaita, A. Benvenuti, F. Pellizzer, and R. Bez, IEEE Trans. Electron Devices **51**, 452 (2004).

[5] V. Weidenhof, I. Friedrich, S. Ziegler, and M. Wuttig, J. Appl. Phys. **89**, 3168 (2001).
[6] D. Ielmini and M. Boniardi, Appl. Phys. Lett. **94**, 091906 (2009).
[7] J. Fortner and J. S. Lannin, Phys. Rev. B **37**, 10154 (1988).
[8] R. De Bastiani, A. M. Piro, M. G. Grimaldi, E. Rimini, G. A. Baratta, and G. Strazzulla, Appl. Phys. Lett. **92**, 241925 (2008).
[9] E. Rimini, R. De Bastiani, E. Carria, M. G. Grimaldi, G. Nicotra, C. Bongiorno, and C. Spinella, J. Appl. Phys. **105**, 123502 (2009).
[10] J. F. Ziegler, J. P. Biresack, and U. Littmark, *The Stopping and the Range of Ions in Solids* (Pergamon, New York, 1985).
[11] K. S. Andrikopoulos, S. N. Yannopoulos, G. A. Voyiatzis, A. V. Kolobov, M. Ribes, and J. Tominaga, J. Phys.: Condens. Matter **18**, 965 (2006).
[12] K. S. Andrikopoulos, S. N. Yannopoulos, A. V. Kolobov, P. Fons, and J. Tominaga, J. Phys. Chem. Solids **68**, 1074 (2007).
[13] H. R. Philipp, J. Non-Cryst. Solids **8-10**, 627 (1972).
[14] M. H. Brodsky, R. J. Gambino, and J. E. Smith, Jr., and Y. Yacoby, Phys. Status Solidi B **52**, 609 (1972).
[15] J. Akola and R. O. Jones, Phys. Rev. B **76**, 235201 (2007).
[16] M. Först, T. Dekorsy, C. Trappe, M. Laurenzis, H. Kurz, and B. Béchevet, Appl. Phys. Lett. **77**, 1964 (2000).
[17] A. Kolobov, P. Fons, A. I. Frenkel, A. L. Ankundinov, J. Tominaga, and T. Uruga, Nature Mater. **3**, 703 (2004).
[18] J. M. Yáñez-Limón, J. González-Hernández, J. J. Alvarado-Gil, I. Delgadillo, and H. Vargas, Phys. Rev. B **52**, 16321 (1995).
[19] S. Privitera, S. Lombardo, C. Bongiorno, E. Rimini, and A. Pirovano, J. Appl. Phys. **102**, 013516 (2007).
[20] Q. M. Lu and M. Libera, J. Appl. Phys. **77**, 517 (1995).
[21] J. Y. Raty, V. V. Godlevsky, J. P. Gaspard, C. Bichara, M. Bionducci, R. Bellissent, R. Céolin, R. Chelikowsky, and Ph. Ghosez, Phys. Rev. B **65**, 115205 (2002).